Breast Cancer Research

Anterior gradient-2 plays a critical role in breast cancer cell growth and survival by modulating cyclin D1, estrogen receptor-alpha and survivin

Breast Cancer Research 2010, **12**:R32 doi:10.1186/bcr2586

Kathryn E Vanderlaag (kathy_vanderlaag@hotmail.com)
Susan Hudak (susan.hudak@spcorp.com)
Laura Bald (laura.bald@spcorp.com)
Laurence Fayadat-Dilman (laurence.fayadat-dilman@spcorp.com)
Manjiri Sathe (manjiri.sathe@spcorp.com)
Jeffery Grein (jeff.grein@spcorp.com)
Mary J Janatpour (mary.janatpour@novartis.com)

ISSN 1465-5411

Article type Research article

Submission date 11 December 2009

Acceptance date 4 June 2010

Publication date 4 June 2010

Article URL http://breast-cancer-research.com/content/12/3/R32

Anterior gradient-2 plays a critical role in breast cancer cell growth and survival by modulating cyclin D1, estrogen receptor-α and survivin

Kathryn E Vanderlaag[1], Susan Hudak[1], Laura Bald[1], Laurence Fayadat-Dilman[1], Manjiri Sathe[1], Jeff Grein[1], Mary J Janatpour[1,2]

[1]Schering-Plough Biopharma, 901 South California Avenue, Palo Alto, CA 94304, USA
[2]Novartis Institutes for BioMedical Research, 4560 Horton Street M/S 4.4, Emeryville, CA 94608, USA

Corresponding author: Mary Janatpour. Email: mary.janatpour@novartis.com

ABSTRACT

Introduction: Anterior-gradient 2 (AGR2) is an estrogen-responsive secreted protein. Its upregulation has been well-documented in a number of cancers, particularly breast cancer for which there is mixed data on the prognostic implications of AGR2 expression. While there is emerging evidence that AGR2 is associated with poor prognosis, its function and impact on cancer relevant pathways has not been elucidated in breast cancer.

Methods: To investigate the biological role of AGR2 in breast cancer, AGR2 was transiently knocked down, using siRNA, in T47D and ZR-75-1 (estrogen receptor-α [ER]-positive) and MDA-MB-231 and SK-BR-3 (ER-negative) human breast cancer cell lines. The impact of silencing AGR2 was evaluated in both anchorage-dependent and anchorage-independent growth (soft agar, spheroid) assays. Cell cycle profiles in ER-positive cell lines were determined by BrdU incorporation and cell death was measured by Annexin V, JC-1 and F7-26 staining. After transiently silencing AGR2 or stimulating with recombinant AGR2, modulation of key regulators of growth and survival pathways was assessed by Western blot. Combination studies of AGR2 knockdown with the antiestrogens tamoxifen and fulvestrant were carried out and assessed at the level of anchorage-dependent growth inhibition and target modulation (cyclin D1, ER).

Results: AGR2 knockdown inhibited growth in anchorage-dependent and anchorage-independent assays, with a more pronounced effect in ER-positive cell lines. Cyclin D1 levels and BrdU incorporation were reduced with AGR2 knockdown. Conversely, cyclin D1 was induced with recombinant AGR2. AGR2 knockdown induced cell death in ZR-

75-1 and T47D cells, and also downregulated survivin and c-Myc. Evidence of AGR2-ER crosstalk was demonstrated by a reduction of ER at the protein level after transiently silencing AGR2. AGR2 knockdown in combination with fulvestrant or tamoxifen did not preclude the efficacy of the antiestrogens, but enhanced it. In addition, p-Src, implicated in tamoxifen resistance, was downregulated with AGR2 knockdown.

Conclusions: Transiently silencing AGR2 in ER-positive breast cancer cell lines inhibited cell growth and cell cycle progression and induced cell death. Breast cancer drivers (ER and cyclin D1) as well as cancer signaling nodes (pSrc, c-Myc and survivin) were demonstrated to be downstream of AGR2. Collectively, the data presented supports the utility of anti-AGR2 therapy in ER-positive breast cancers due to its impact on cancer relevant pathways.

INTRODUCTION

In the United States, 1 in 8 women will be diagnosed with breast cancer in their lifetime and the incidence is rising worldwide [1]. Estrogen receptor-α (ER) positive breast cancer accounted for 75% of breast cancer cases in the US between 1992-1998 [2]. 17β-estradiol (E2) is the ligand for ER and exerts its action by upregulating a number of key mediators including cyclin D1 and c-Myc [3,4]. Cyclin D1 is overexpressed in over 50% and amplified in 15% of breast cancer cases [5] and acts as a mitogenic sensor [6] by responding to oncogenes and various growth factors including E2. It plays a critical role in cell cycle progression, as evidenced by the lack of entry into S phase in the absence of cyclin D1 [7]. In addition, cyclin D1 deficient mice do not grow breast tumors when induced by the oncogenes Ras and Neu [8], further supporting cyclin D1 as a key driver in certain breast tumors.

Due to its impact on cell growth and survival pathways, E2 signaling has proven to be an efficacious target for ER-positive breast cancer therapy. However, approximately half of ER-positive tumors have an intrinsic resistance to endocrine therapy and 30-40% of the remaining responsive population will acquire resistance to tamoxifen [9], thus necessitating the exploration of alternative therapeutic targets.

Anterior gradient-2 (AGR2) is a secreted protein that was originally identified to be co-expressed with ER in breast cancer cell lines [10]. AGR2 has since been demonstrated to be estrogen [11-13] and androgen-responsive [14] and its upregulation has been reported in a number of cancers including breast, lung, ovarian, gastric, pancreatic, esophageal and prostate cancer [11,15-25]. Additionally, in the ER-negative breast cancer cell line, MDA-MB-231, AGR2 was induced under serum-starvation and hypoxia [26], suggesting a role for AGR2 in physiologically relevant stress conditions.

Early expression studies have correlated AGR2 expression with a better prognosis [18], possibly due to its positive association with ER-positive tumors, which typically have a more favorable prognosis than their ER-negative counterparts [27]. Subsequent studies have since explored within the ER-positive tumor population and shown that AGR2 is inversely associated with overall and relapse-free survival [21,25], prompting us to ask whether AGR2 plays a critical role in more invasive ER-positive tumors.

Literature relating to AGR2's functional role in cancer is limited in scope. In the premalignant Barrett's esophagus and esophageal cancer models, AGR2 overexpression induces colony formation and transformation [15,28]. While in the course of this investigation, the converse, siRNA or shRNA – mediated AGR2 knockdown, was shown to inhibit colony and sub-cutaneous growth in esophageal and pancreatic cancer models [24,28]. In breast cancer models, overexpression of AGR2 failed to alter tumor formation in vivo or growth rate in vitro, but, rather, reduced cell adhesion and increased the number of metastases [11]. While the phenotypic observations in these papers are compelling, very little signaling downstream of AGR2 has been elucidated.

AGR2 warranted further evaluation of its biology based collectively on its prevalence in breast cancer, its negative correlation with patient survival within the ER-positive breast cancer sub-population and literature implications of a functional role in cancer. To evaluate the impact of targeting AGR2 in cancer, siRNA was utilized to knockdown AGR2 in breast cancer cell lines that endogenously express AGR2 at varying levels. Phenotypic effects on cell proliferation and death, as well as modulation of key cancer signaling nodes, including cyclin D1, c-Myc, p-Src and survivin, were observed. These pathways were conversely modulated upon treatment of a breast cancer line with recombinant AGR2. Combining AGR2 knockdown with ER antagonists

resulted in enhanced anti-proliferative effects on ER-positive lines. Altogether our results demonstrate a critical role for AGR2 in breast cancer growth and survival, identify downstream signaling of AGR2 and thus support AGR2 as a promising oncology target for therapeutic agents.

MATERIALS AND METHODS

Cell lines and chemicals. Human breast cancer cell lines T47D, ZR-75-1, MCF-7, MDA-MB-231 and SKBR3 were purchased from ATCC. Cell lines were maintained per ATCC guidelines. The cells were grown at 37°C in a humidified atmosphere with 5% CO_2. 17β-estradiol, ICI 182,780, MG132, 4-hydroxytamoxifen were obtained from Sigma. Propidium iodide/RNase solution was purchased from BD Biosciences.

Detection of AGR2 in supernatant. Conditioned media from cell lines was collected and centrifuged to remove cell debris. AGR2 was immunoprecipitated (IP) from 2 mL samples with Protein A/G beads, 40 ug mouse anti-AGR2 (Novus) or isotype control and overnight incubation. IP samples were analyzed by Western blot (described below).

siRNA knockdown. Cells were transfected in Optimem (Gibco) containing 100nM siRNA pools using Dharmafect 3 (Dharmacon) for SK-BR-3 cells or Dharmafect 4 for all other cell lines for 24 hours according to the manufacturer's protocol. Invitrogen AGR2 pooled siRNA, Invitrogen stealth negative control, KSP positive control (Dharmacon) or Dharmacon negative control siRNA were used. To support the effects observed after siRNA knockdown in Figures 1-6 as being AGR2-specific effects and not an off-target effect of the Invitrogen siRNA reagent, additional AGR2 siRNA reagents were employed. siRNA reagents targeting distinct sequences from Ambion (Ambion Silencer) and Dharmacon (On-Target Plus Smartpool) were used in anchorage-dependent functional

studies in T47D and MDA-MB-231 cells with similar effects as seen with the Invitrogen reagent (see Supplementary figure S1a in Additional file 1).

Cell Titer Glo viability assay. Twenty-four hours after transfection, $5x10^3$ cells were plated in black view plates. Cell Titer Glo reagent (Promega) was added according to the manufacturer's directions 96h post-transfection. The luminescence was read with a multiwell plate reader (DTX 880) and an integration time of 100,000μs.

Soft agar colony formation assay. 96-well flat bottom plates were coated with 1% agarose. Twenty-four hours after transfection, 5×10^2 cells/well were added in media with a final concentration of 0.33% agarose. After a 7-day incubation, Alamar blue (Biosource) was added to each well and the fluorescence was read using a multiwell plate reader at 530/590 nm.

Spheroid assay. Twenty-four hours after transfection, cells were plated at a density of $1x10^4$ cells/well in 96-well round bottom plates coated with Polyhema (Sigma) and grown on a waver platform. The spheroids were lysed in a final concentration of 2% Triton X-100 after 7 days. The LDH kit (Promega) was used according to the manufacturer's directions for lysed spheroids and read on a plate reader at 560/590 nm.

Cell cycle analysis by BrdU incorporation. Cell cycle analysis was determined by transfecting cells with siRNA, harvesting (adherent and suspension) cells after 48h and measuring BrdU incorporation as previously described [29]. Samples were then analyzed using a FACSCanto (Becton Dickinson) and FlowJo was used to quantitate the cell cycle distribution.

Detection of cell death by Annexin V/Propidium Iodide staining. Cells were plated at a density of $1x10^5$ cells/mL and treated with AGR2 siRNA for 96 h. Floating and adherent cells were stained with Annexin V-Alexa Fluor 488 (Invitrogen) as described in

the manufacturer's protocol and resuspended in PI/RNase. Samples were run within 30 minutes by flow cytometry and plots were analyzed in FlowJo.

Detection of ssDNA breaks by F7-26 staining. Detection of apoptosis was determined 96h after AGR2 siRNA treatment by collection of floating and adherent cells and fixation in 100% methanol overnight. Cells were then stained for F7-26 as previously described [30]. Cells were resuspended in PI/RNase solution and analyzed using a FACSCanto. FACS plots were analyzed in FlowJo.

Measurement of mitochondrial membrane potential by JC-1. Cells were plated at a density of $1x10^5$ cells/6-well plate and were harvested 96h after AGR2 siRNA treatment. Cells were stained with JC-1 (Invitrogen) according to the manufacturer's directions, including the positive control CCCP. Samples were analyzed using a FACSCanto and CCCP-treated samples were used to perform standard compensation. The ratio of JC-$1_{aggregate}$/JC-$1_{monomer}$ was determined by calculating the geometric mean of PE/FITC in FlowJo and then expressed as a ratio of the untransfected control population.

Western blot analysis. Lysates was isolated using the RIPA buffer (Sigma) containing phosphatase and protease inhibitors according to the manufacturer's directions. Western blot analyses were done in 2-5% milk-0.05% TBS-Tween at a dilution of 1:1000 overnight at 4°C. Antibodies were purchased from the following vendors: Novus (AGR2), Santa Cruz Biotechnology (ER), Epitomics (cyclin D1, c-Myc), Cell Signaling (cyclin D1, E2F1, p-Erk, Erk, p-Src, Src, survivin). Secondary conjugated sheep anti-mouse IgG (Amersham) and donkey anti-rabbit IgG (Amersham) HRP antibodies were used at 1:5000 for an hour. Blots were developed using chemiluminescent reagents (Pierce). Densitometry was performed on cyclin D1, ER and β-actin bands using ImagePro (NIH) and a ratio of cyclin D1 or ER values to loading control (β-actin) values

for each treatment were computed. Ratios were expressed relative to untransfected samples from the same timepoint.

Treatment of ZR-75-1 cells with E2. ZR-75-1 cells were plated at a density of $1.25x10^5$ cells/mL in RPMI containing 2% charcoal-stripped serum. Twenty-four hours after plating, media was removed and E2 was then added at a final concentration of 10 nM and protein was isolated after 24h as described previously.

Cyclin D1 detection in ZR-75-1 cells treated with rhAGR2. ZR-75-1 cells were plated in 6-well plates or Lab-Tek II chamber slides (Nalge Nunc) in reduced serum and treated with 5 ug/mL of BSA, rhAGR2 (in-house) or full-length rhAGR2 (Novus). Protein from 6-well plates was isolated 6h after treatment as described previously. Slides were fixed 6h after rhAGR2 treatment with 10% neutral buffered formalin, blocked in 3% BSA + 0.5% Triton X in PBS, incubated overnight with anti-cyclin D1 Ab (Epitomics), 1:200, and for 1h with Alexa 594-Goat anti-rabbit (Invitrogen), 1:500. Slides were mounted using Pro-Long Gold with DAPI and the slides were imaged with a fluorescent microscope (Leica). Quantitation of cyclin D1 intensity was performed using ImagePro by generating a DAPI-based nuclear map and determining the relative cyclin D1 intensity per nucleus, which was subsequently separated into 4 bins based on relative intensity. In-house rhAGR2 was purified from mammalian HEK293E cells overexpressing N-terminal His-tagged recombinant AGR2.

E2 and/or antiestrogen treatment. T47D cells were plated at a density of $1 x10^5$ cells/mL in 10% charcoal-stripped RPMI and transfected as previously described. 24h post-transfection, media was changed to 5% charcoal-stripped RPMI and cells for functional assays were replated at a density of $3x10^3$ cells/well for Cell Titer Glo and treated with vehicle, E2 or antiestrogens. Protein was isolated 72h post-transfection and phenotype plates were assayed 96-120h post-transfection.

Generation of monoclonal rat anti-AGR2 Ab and test of AGR2 Ab specificity and cross-reactivity by ELISA. One Lewis rat was immunized with human recombinant AGR2 generated in-house for 4 months. The inguinal and popliteal nodes were subsequently harvested and fused by electrofusion using Cyto PulseSciences Model PA-101C Electrofusion System. To test for specificity and cross-reactivity, mouse AGR2, human AGR2 and AGR3 ELISAs were employed. Plates were coated with in-house human AGR2, human AGR3 or mouse AGR2 at 0.5ug/mL (50 uL total volume in PBS) overnight at 4^{o}C. Supernatant from fusions (50uL) were incubated on coated plates for 1h at room temperature, followed by 1:2000 of goat anti-rat HRP Ab (Jackson Laboratories) for 30 minutes at room temperature. ABTS (50uL/well) was added to wells and incubated for 10 minutes at room temperature. Absorbance was read at 405nm.

Anti-AGR2 Ab treatment of T47D cells. Cells were plated in 96 well flat bottom plates at 1000 cells/well for growth assays or Lab-Tek II chamber slides in low (2%) serum for cyclin D1 immunofluorescence studies. Cell plated in chamber slides were treated with the rat anti-AGR2 Ab generated in-house twice in a 48h period at a concentration of 10ug/mL and stained for cyclin D1 as previously described. For growth studies, forty-eight hours after plating, antibodies were added to 96-well plates at a final concentration of 20ug/ml. After an additional 5 days of incubation, MTT Reagent (Roche) was added according to the manufacturer's instructions. After four hours Lysis Buffer was added and plates were incubated an additional twenty-four hours. Plates were read using a multi-well plate reader at 550/690nm.

Statistical analysis. A two-tailed Student's *t* test was used for statistical analysis of comparative data using GraphPad Prism. Data were expressed as means of at least three independent experiments ± SD, with $P < 0.05$ considered statistically significant.

RESULTS

AGR2 knockdown in breast cancer cells impacts anchorage-dependent and anchorage-independent growth. Previous reports have shown that knocking down AGR2 has an impact on growth in esophageal and pancreatic cancer cell lines [24,28]. The role of endogenous AGR2 in breast cancer cell proliferation was assessed by anchorage-dependent and anchorage-independent growth assays. Four breast cancer cell lines, two ER-positive (T47D and ZR-75-1) and two ER-negative (MDA-MB-231, SK-BR-3) were utilized. All cell lines were transiently transfected with siControl and siAGR2. Endogenous AGR2 expression was detected in cell line supernatants and whole cell lysates (Figure 1a) and knockdown of AGR2 protein (Figure 1a, right) was confirmed up to 96h after transfection (Supplementary figure S1b in Additional file 1). Silencing AGR2 inhibited anchorage-dependent proliferation and anchorage-independent spheroid growth only in ER-positive cell lines (Figure 1b,d). Similar results on anchorage-dependent growth in ER-positive T47D and ER-negative MDA-MB-231 cells were obtained using multiple AGR2 siRNA reagents that targeted distinct sequences (Supplementary figure S1a in Additional file 1). In all 4 cell lines, AGR2 knockdown inhibited anchorage-independent growth in the soft agar assay (Figure 1c). Collectively, this data demonstrates that AGR2 knockdown has a negative impact on anchorage-dependent and anchorage-independent growth that is more pronounced in ER-positive breast cancer cells.

AGR2 knockdown has an impact on cell cycle and induces cell death. To determine if the phenotype from Figure 1 was a result of growth inhibition and/or cell death, cell cycle profiles and apoptosis/necrosis assays were utilized. In T47D and ZR-

75-1 cells, transient knockdown of AGR2 significantly reduced the percentage of cells in S phase >40% and increased the percentage of cells in G_0/G_1 phase compared to the transfection control (Figure 2a, 2b). By contrast, treatment with siAGR2 in the two ER-negative cell lines, MDA-MB-231 and SK-BR-3 cells, failed to alter the cell cycle profile compared to control cells (Figure 2c, 2d).

Transient knockdown of AGR2 in ZR-75-1 cells yielded an 11% increase in F7-26 staining, indicative of single-stranded DNA breaks and apoptosis (Figure 3a). An apoptotic phenotype upon AGR2 knockdown in ZR-75-1 cells was further supported by an observed depolarization of the mitochondrial membrane, established using JC-1 staining, that was comparable to the apoptosis-inducing control, MG132 (Figure 3b). By contrast, in T47D cells, AGR2 silencing increased the percentage of the propidium-iodide-only cell population >7% above both the negative control and apoptosis control, which is indicative of necrosis. Although the increase in propidium iodide staining was moderate, we consistently observed this result (n=3). The Annexin V positive population was only slightly higher compared to control samples after AGR2 knockdown (Figure 3c). In T47D cells, JC-1 staining indicated a hyperpolarization of the mitochondrial membrane after knocking down AGR2 (Figure 3d), which is required for distinct stages of both apoptosis and necrosis [31]. In apoptosis, hyperpolarization occurs early and is followed by depolarization, which was not observed at later timepoints in siAGR2-treated T47D cells (Supplementary figure S2b in Additional file 2), whereas sustained hyperpolarization has been reported to sensitize cells to necrosis [32]. Furthermore, consistent with necrotic, non-apoptotic, cell death in T47D cells, there was no increase in the F7-26 positive population after AGR2 knockdown (Supplementary figure S2a in Additional file 2). Based on BrdU incorporation and death assays, AGR2 knockdown in

ER-positive, but not ER-negative, cells reduces cell proliferation and induces cell context-dependent death.

AGR2 modulates critical regulators of cell growth and survival. To dissect the signaling associated with the cell death and cell cycle phenotypes observed in Figures 2 and 3, the impact of AGR2 knockdown on critical regulators of these pathways were assayed by Western blot. In T47D and ZR-75-1 cells, the protein c-Myc and the anti-apoptotic protein survivin were reduced after AGR2 knockdown (Figure 4a), consistent with the cell death effects observed in Figure 3. To a lesser degree, survivin was also downregulated in SK-BR-3 cells treated with siAGR2. Since knockdown of AGR2 in ER-positive cells yielded an accumulation of cells in G_0/G_1, key regulators of this phase of the cell cycle were assayed by Western blot in these cell types. Interestingly, in all 4 cell types tested, cyclin D1 protein were downregulated with AGR2 silencing (Figure 4a). In addition, E2F1 was downregulated in T47D, ZR-75-1 and MDA-MB-231 and was also consistently downregulated to a modest degree in SK-BR-3 cells (n=3). Given that AGR2 is secreted (Figure 1), we asked whether it could act extracellularly. When ZR-75-1 cells were treated with recombinant AGR2 (Figure 4b-d), cyclin D1 was induced, beyond already significant levels, confirming that cyclin D1 is downstream of AGR2.

Evidence of AGR2-ER crosstalk. Previous studies have shown that E2 treatment in MCF-7 cells induces AGR2 at the message level [11]. Consistent with AGR2 responsiveness to E2, E2 treatment in ZR-75-1 cells further induced AGR2 at the protein level (Figure 5a). We subsequently investigated potential crosstalk between AGR2 and ER since E2 signaling impacts the cell cycle, c-Myc and cyclin D1 [33], which are also modulated with AGR2 knockdown. Notably, there have been numerous reports of ER crosstalk with other pathways [34-36]. To determine if AGR2 could conversely impact E2 signaling, ER levels were assessed after AGR2 knockdown. In ER-positive cells,

silencing of AGR2 yielded a reduction of ER protein (Figure 5b). In T47D cells, a double band for ER was detected, which may be due to a phosphorylated form of the protein. Collectively, these data suggest that E2 can impact AGR2 protein levels and, conversely, knockdown of AGR2 can lead to a reduction in ER protein levels.

AGR2 biology involves ER-dependent and ER-independent mechanisms. Much of the AGR2 biology shown thus far might be tied to an impact on ER and subsequent downstream signaling. The partial antiestrogen, tamoxifen, and 'pure' antiestrogen, fulvestrant - first line treatments for ER-positive patients - both modulate cell cycle and reduce cyclin D1 and c-Myc levels [33]. In addition, in similar fashion to AGR2 knockdown, ER is downregulated by fulvestrant. Therefore we wanted to determine how AGR2 knockdown might impact antiestrogen activity. Phenotypically, AGR2 knockdown augmented the degree of growth inhibition when combined with either antiestrogen (Figure 6a). At the level of target modulation, silencing AGR2 in combination with antiestrogens further enhanced ER and cyclin D1 downregulation (Figure 6b, compare lane 6 to lanes 9 and 12). This suggests that anti-AGR2 therapy would not preclude the activity of an antiestrogen and the combination may be advantageous.

Tamoxifen treatment in MCF-7 cells has been reported to elevate Src phosphorylation levels and is associated with acquired tamoxifen resistance [37]. Recently, targeting both Src and ER has been shown to prevent acquired resistance to tamoxifen therapy [38]. To determine if inhibiting AGR2 activity might impact this resistance-associated protein, phosphorylation of Src was examined. Silencing AGR2 downregulated p-Src, but not total Src levels, in both ER-positive breast cancer cell lines (Figure 6c).

Since cyclin D1 is a downstream target of E2 signaling, we sought to determine if cyclin D1 modulation by AGR2 could be tied exclusively to an impact on ER. The

kinetics of AGR2 knockdown was assessed at 24, 32 and 48h. Cyclin D1 was downregulated after 24h, whereas ER was downregulated at 32h (Figure 6d), indicating that cyclin D1 downregulation was at least, in part, due to an ER-independent mechanism. This is also consistent with cyclin D1 downregulation observed in ER-negative cell lines (Figure 4a).

Anti-AGR2 Ab modulates cyclin D1 and inhibits cell growth. While the induction of cyclin D1 protein with recombinant AGR2 suggested that AGR2 can act extracellularly (Figure 4c), given that Park et al. had shown that AGR2 is an endoplasmic reticulum protein [39], we asked whether AGR2 activity could be inhibited extracellularly. Monoclonal antibodies raised in rats immunized with recombinant AGR2 were assayed for AGR2 specificity and species cross-reactivity by ELISA. The antibody shown bound both mouse and human forms of AGR2, but not human AGR3 (Figure 7a). Cultured T47D cells were treated with the monoclonal Ab and compared to AGR2 siRNA treatment for effects on cyclin D1, using cyclin D1 immunofluorescence staining (Figure 7b, left panel). Images were quantitated for relative cyclin D1 intensity (Figure 7b, right panel). Consistent with Western data (Fig 4a), cyclin D1 was reduced after transiently silencing AGR2 by siRNA in T47D cells. Cyclin D1 was also significantly reduced in T47D cells treated with an anti-AGR2 antibody. The impact of the AGR2 Ab on cell growth was investigated in T47D, ZR-75-1 and MDA-MB-231 cells. Treatment with the anti-AGR2 Ab modestly reduced cell growth in all 3 cell lines. In summary, the effects of the anti-AGR2 Ab suggest that AGR2 can act extracellularly.

DISCUSSION

AGR2 is overexpressed in a number of epithelial cancers [11,15-25] and is inversely associated with patient survival in the ER-positive patient population [21,25].

While this association itself does not indicate a critical role for AGR2 in disease progression, it does warrant examination of functional relevance of this gene. Both anchorage-dependent and anchorage-independent growth were inhibited after silencing endogenously-expressed AGR2 in ER-positive cell lines (Figure 1). This impact on growth was seen with multiple AGR2 siRNA sequences (Supplementary figure S1 in Additional file 1), which supports the specificity of the effect of AGR2 knockdown on the inhibition of cancer cell growth. AGR2 knockdown significantly reduced colony formation in soft-agar in ER-negative lines, as well (Figure 1c), raising an interesting discrepancy between ER-positive and ER-negative lines. The soft agar assay represents a particularly stressful in vitro assay, as it requires the cancer cells to grow from a single cell, whereas other assays allow for cell-cell interaction. There is support in the literature for a role of AGR2 in stress conditions [15,26]. Another possibility is that the soft agar assay measures AGR2-dependent biologies that are not captured in the other assays, a concept which is consistent with distinct breast cancer models, where AGR2 overexpression was reported to play a role in metastases and adhesion, but not growth [11]. Aligned with the hypothesis that MDA-MB-231 cells may be more sensitive to neutralization of AGR2 activity under stress conditions, we observed that our AGR2 neutralizing mAb inhibited MDA-MB-231 cell growth under low serum conditions. As noted above, siRNA-mediated knockdown of AGR2 in MDA-MB-231 cells in full serum conditions had little growth effect in anchorage dependent conditions. In fact, the MDA-MB-231 cells were more sensitive to growth inhibition with the AGR2-neutralizing mAb than T47D and ZR-75-1 cells, although this may be trivially explained by the observation that MDA-MB-231 cells have significantly lower levels of AGR2 than T47D and ZR-75-1 cells used in the same experiment and thus may be more readily neutralized. While this is the first time a role for AGR2 has been demonstrated in breast cancer cell growth,

these results are consistent with the impact of AGR2 knockdown on cell growth reported in other non-breast cancer models.

To further evaluate the role of AGR2 in breast cancer, the impact on cell death and cell cycle were explored. Supporting the anchorage-dependent functional data, a cell cycle phenotype and induction of cell death was seen in both T47D and ZR-75-1 cells (Figures 2,3). Thus far, neither phenotype has been previously reported. The BrdU phenotype is in contrast to previous reports where stable expression of AGR2 in H1299 cells had no effect on the cell cycle or DNA synthesis [15]. There were cell context-dependent differences in the mechanisms of cell death, which may be related to the genetic background of the respective cell lines, such as the differences in p53 status, but cell death was observed in either case. That inhibition of AGR2 activity can induce cytotoxicity, in addition to being cytostatic, is particularly important for the potential to treat slow-growing tumors.

To provide support for the phenotypic effects shown with AGR2 knockdown and understand AGR2 biology in greater depth, we investigated intracellular signaling downstream of AGR2. Mechanistic hints from the literature have been limited to a role for AGR2 in the wild-type p53 transcriptional response [15]. Since T47D cells have mutated p53 and ZR-75-1 cells have wild type p53 and a phenotype with AGR2 knockdown was observed in both, AGR2 biology cannot be limited to the p53 pathway. Cell cycle modulation and induction of cell death after transient knockdown of AGR2 directed us to explore other signaling pathways that may be relevant to AGR2 biology. Modulation of cyclin D1, c-Myc and E2F1 by AGR2 knockdown is consistent with the cell cycle and anchorage-dependent growth phenotype seen in the ER-positive cell lines. The impact of AGR2 knockdown on cyclin D1 in ER-negative cell lines that did not translate into a cell cycle phenotype was an intriguing result. There are several

possibilities that could account for this observation. It could also be a threshold issue, requiring that a certain percentage of cyclin D1 be downregulated in order to result in a phenotype similar to that observed in ER-positive cells. It is of note that cyclin D1 can be downregulated through both ER-dependent and ER-independent pathways. In addition, ZR-75-1 cells have cyclin D1 amplified and are known to be driven by cyclin D1 [40], which may not be as key a driver in the ER-negative cell types tested. Collectively, downregulation of cyclin D1 in all 4 cell types after AGR2 knockdown or treatment with an anti-AGR2 Ab supports cyclin D1 being downstream of AGR2.

We also provide evidence that AGR2 can act extracellularly. This finding is in contrast to a recent report suggesting that AGR2, a member of the protein disulfide isomerase family, is localized in the endoplasmic reticulum and plays an essential role for mucus production [39]. Since cyclin D1 is induced with an exogenous source of AGR2 (Figure 4) and reduced with an anti-AGR2 Ab (Figure 7), and AGR2 is detected in the supernatant of breast cancer cell lines, it suggests that AGR2 may have an extracellular mechanism of action. Consistent with our data, other disulfide isomerases have also been associated with cancer-relevant biologies including invasiveness and stress survival [41,42].

To provide further evidence that AGR2 is important in breast cancer progression, silencing AGR2 in ER-positive cells downregulated c-Myc, p-Src and survivin. All of these molecules play critical roles in breast cancer progression by impacting growth, survival, angiogenesis, migration and invasion [43] and hence are individually being investigated as targeted monotherapies [44,45]. Given the high level of biological relevance of p-Src, survivin and c-Myc in cancer, modulation of these key players after silencing AGR2 suggests AGR2 may be key in other cancers, beyond breast cancer.

E2 is another key driver and potent mitogen of breast cancer. Several papers in the literature indicate AGR2 is an E2-responsive gene [11-13] and we similarly observed an induction of AGR2 in E2-treated ZR-75-1 cells (Figure 5a). The more novel finding is that ER protein levels are reduced after AGR2 knockdown (Figure 5b). Since ER downregulation leads to reduced estrogen responsiveness with fulvestrant, this suggests that ER downregulation induced by AGR2 knockdown might also negatively influence the mitogenic activity of E2. The relative E2 responsiveness could not be accurately assessed in these AGR2-silenced cells given the complexity of the relationships of these molecules since E2 itself modulates ER in T47D cells [46].

Given the similar profiles of AGR2 knockdown with E2 signaling, there were important considerations when assessing the potential crosstalk between the ER and AGR2 pathways. Initially, we asked how AGR2 knockdown would impact the effect of antiestrogens on cancer cell lines. Next, we determined whether AGR2 may have ER-independent activities. AGR2 knockdown in combination with antiestrogens did not preclude antiestrogen efficacy and the combination enhanced the impact on growth, ER and cyclin D1 (Figure 6a, 6b). The kinetics of AGR2 knockdown showed that cyclin D1 downregulation occurs prior to ER downregulation and therefore AGR2 has an ER-independent pathway for downregulating cyclin D1, which is supported by the impact on cyclin D1 seen in ER-negative cells.

CONCLUSIONS

AGR2 is commonly overexpressed in cancers and our data suggests an important functional role for AGR2 in breast cancer. AGR2 impacts key breast cancer drivers including cyclin D1, c-Myc and ER, as well as more general oncogenic signaling nodes such as p-Src and survivin. Removal of AGR2 has an impact on cancer relevant

pathways including the cell cycle and E2 signaling, ultimately resulting in cell death; thus demonstrating that AGR2 plays a critical role in breast cancer progression. Beyond elucidating novel biology, the mechanism of action also suggests that AGR2 would be a good therapeutic target since its inhibition appears to have added benefit when combined with conventional antiestrogen treatments. Tumors treated with tamoxifen can become hypersensitive to E2 [47] and both an anti-AGR2 therapy and fulvestrant address this issue since ER is downregulated with these treatments. In addition, survivin and p-Src have been implicated in tamoxifen resistance and both are modulated by AGR2 knockdown. Furthermore, an anti-AGR2 therapy, unlike fulvestrant, can potentially function in cancers driven by cyclin D1 that can no longer respond to E2 given AGR2's ER-independent actions on cyclin D1. Collectively, the data presented supports the utility of an anti-AGR2 therapy in ER-positive breast cancers.

ABBREVIATIONS

Ab=antibody; AGR2=anterior gradient-2; E2=17-beta-estradiol; ER=estrogen receptor-alpha; IP=immunoprecipitation. rh=recombinant human.

COMPETING INTERESTS

The authors declare that Schering-Plough has a patent that includes data from this manuscript.

AUTHORS' CONTRIBUTIONS

KV drafted manuscript, performed cell cycle experiments and initiated cell death, rhAGR2 stimulation and ER-AGR2 crosstalk experiments. SH performed numerous functional experiments and observed cyclin D1, p-Src proteins modulated after knocking

down AGR2 in breast cancer cells. LB generated anti-AGR2 Ab and performed ELISAs. JG profiled cell lines for AGR2 mRNA expression, which led to the selection of cell lines for the experiments carried out. LF expressed and purified AGR2 protein used in rhAGR2 stimulation experiments. MS carried out Taqman analysis of a panel of genes in AGR2-silenced samples, which led to the observation of a downregulation of cyclin D1. MJJ initiated and oversaw the AGR2 project, devised key experiments and edited the manuscript.

ACKNOWLEDGEMENTS

We thank Enrique Escandon (Schering-Plough Biopharma) for careful review of the manuscript.

REFERENCES

1. SEER Cancer Statistics Review, 1975-2005, National Cancer Institute [http://seer.cancer.gov/csr/1975_2005/]

2. Anderson WF, Chatterjee N, Ershler WB, Brawley OW: Estrogen receptor breast cancer phenotypes in the Surveillance, Epidemiology, and End Results database. *Breast Cancer Res Treat* 2002, 76:27-36.

3. Dubik D, Shiu RP: Mechanism of estrogen activation of c-myc oncogene expression. *Oncogene* 1992, 7:1587-94.

4. Altucci L, Addeo R, Cicatiello L, Dauvois S, Parker MG, Truss M, Beato M, Sica V, Bresciani F, Weisz A: 17beta-Estradiol induces cyclin D1 gene transcription, p36D1-p34cdk4 complex activation and p105Rb phosphorylation during mitogenic stimulation of G(1)-arrested human breast cancer cells. *Oncogene* 1996, 12:2315-24.

5. Gillett C, Fantl V, Smith R, Fisher C, Bartek J, Dickson C, Barnes D, Peters G: Amplification and overexpression of cyclin D1 in breast cancer detected by immunohistochemical staining. *Cancer Res* 1994, 54:1812-7.

6. Diehl JA: Cycling to cancer with cyclin D1. *Cancer Biol Ther* 2002, 1:226-31.

7. Matsushime H, Quelle DE, Shurtleff SA, Shibuya M, Sherr CJ, Kato JY: D-type cyclin-dependent kinase activity in mammalian cells. *Mol Cell Biol* 1994, 14:2066-76.

8. Yu Q, Geng Y, Sicinski P: Specific protection against breast cancers by cyclin D1 ablation. *Nature* 2001, 411:1017-21.

9. Ring A, Dowsett M: Mechanisms of tamoxifen resistance. *Endocr Relat Cancer* 2004, 11:643-58.

10. Thompson DA, Weigel RJ: hAG-2, the human homologue of the Xenopus laevis cement gland gene XAG-2, is coexpressed with estrogen receptor in breast cancer cell lines. *Biochem Biophys Res Commun* 1998, 251:111-6.

11. Liu D, Rudland PS, Sibson DR, Platt-Higgins A, Barraclough R: Human homologue of cement gland protein, a novel metastasis inducer associated with breast carcinomas. *Cancer Res* 2005, 65:3796-805.

12. Wilson CL, Sims AH, Howell A, Miller CJ, Clarke RB: Effects of oestrogen on gene expression in epithelium and stroma of normal human breast tissue. *Endocr Relat Cancer* 2006, 13:617-28.

13. Mackay A, Urruticoechea A, Dixon JM, Dexter T, Fenwick K, Ashworth A, Drury S, Larionov A, Young O, White S, Miller WR, Evans DB, Dowsett M: Molecular

response to aromatase inhibitor treatment in primary breast cancer. *Breast Cancer Res* 2007, 9:R37.

14. Zhang JS, Gong A, Cheville JC, Smith DI, Young CY: AGR2, an androgen-inducible secretory protein overexpressed in prostate cancer. *Genes Chromosomes Cancer* 2005, 43:249-59.

15. Pohler E, Craig AL, Cotton J, Lawrie L, Dillon JF, Ross P, Kernohan N, Hupp TR: The Barrett's antigen anterior gradient-2 silences the p53 transcriptional response to DNA damage. *Mol Cell Proteomics* 2004, 3:534-47.

16. Kristiansen G, Pilarsky C, Wissmann C, Kaiser S, Bruemmendorf T, Roepcke S, Dahl E, Hinzmann B, Specht T, Pervan J, Stephan C, Loening S, Dietel M, Rosenthal A: Expression profiling of microdissected matched prostate cancer samples reveals CD166/MEMD and CD24 as new prognostic markers for patient survival. *J Pathol* 2005, 205:359-76.

17. Shen D, Chang HR, Chen Z, He J, Lonsberry V, Elshimali Y, Chia D, Seligson D, Goodglick L, Nelson SF, Gornbein JA: Loss of annexin A1 expression in human breast cancer detected by multiple high-throughput analyses. *Biochem Biophys Res Commun* 2005, 326:218-27.

18. Fritzsche FR, Dahl E, Dankof A, Burkhardt M, Pahl S, Petersen I, Dietel M, Kristiansen G: Expression of AGR2 in non small cell lung cancer. *Histol Histopathol* 2007, 22:703-8.

19. Fritzsche FR, Dahl E, Pahl S, Burkhardt M, Luo J, Mayordomo E, Gansukh T, Dankof A, Knuechel R, Denkert C, Winzer KJ, Dietel M, Kristiansen G: Prognostic relevance of AGR2 expression in breast cancer. *Clin Cancer Res* 2006, 12:1728-34.

20. Kovalev LI, Shishkin SS, Khasigov PZ, Dzeranov NK, Kazachenko AV, Kovaleva MA, Toropygin I, Eremina LS, Grachev SV: [New approaches to molecular diagnosis of prostatic cancer]. *Urologiia* 2006,16-9.

21. Innes HE, Liu D, Barraclough R, Davies MP, O'Neill PA, Platt-Higgins A, de Silva Rudland S, Sibson DR, Rudland PS: Significance of the metastasis-inducing protein AGR2 for outcome in hormonally treated breast cancer patients. *Br J Cancer* 2006, 94:1057-65.

22. Zhang Y, Forootan SS, Liu D, Barraclough R, Foster CS, Rudland PS, Ke Y: Increased expression of anterior gradient-2 is significantly associated with poor survival of prostate cancer patients. *Prostate Cancer Prostatic Dis* 2007, 10:293-300.

23. Zhu H, Lam DC, Han KC, Tin VP, Suen WS, Wang E, Lam WK, Cai WW, Chung LP, Wong MP: High resolution analysis of genomic aberrations by metaphase and array comparative genomic hybridization identifies candidate tumour genes in lung cancer cell lines. *Cancer Lett* 2007, 245:303-14.

24. Ramachandran V, Arumugam T, Wang H, Logsdon CD: Anterior gradient 2 is expressed and secreted during the development of pancreatic cancer and promotes cancer cell survival. *Cancer Res* 2008, 68:7811-8.

25. Wu ZS, Wu Q, Ding XD, Wang HQ, Shen YX, Fang SY: [Expression of a novel metastasis-inducing protein human anterior gradient-2 (AGR2) in breast cancer and its clinical and prognostic significance]. *Zhonghua Bing Li Xue Za Zhi* 2008, 37:109-13.

26. Zweitzig DR, Smirnov DA, Connelly MC, Terstappen LW, O'Hara SM, Moran E: Physiological stress induces the metastasis marker AGR2 in breast cancer cells. *Mol Cell Biochem* 2007, 306:255-60.

27. Kamby C, Rose C, Iversen H, Holm NV, Andersen KW, Thorpe SM: [The pattern of metastases in breast cancer and the relation to estrogen receptor status]. *Ugeskr Laeger* 1986, 148:2546-8.

28. Wang Z, Hao Y, Lowe AW: The adenocarcinoma-associated antigen, AGR2, promotes tumor growth, cell migration, and cellular transformation. *Cancer Res* 2008, 68:492-7.

29. Cho SH, Toouli CD, Fujii GH, Crain C, Parry D: Chk1 is essential for tumor cell viability following activation of the replication checkpoint. *Cell Cycle* 2005, 4:131-9.

30. Frankfurt OS: Detection of apoptosis in leukemic and breast cancer cells with monoclonal antibody to single-stranded DNA. *Anticancer Res* 1994, 14:1861-9.

31. Skulachev VP: Bioenergetic aspects of apoptosis, necrosis and mitoptosis. *Apoptosis* 2006, 11:473-85.

32. Gergely P, Jr., Grossman C, Niland B, Puskas F, Neupane H, Allam F, Banki K, Phillips PE, Perl A: Mitochondrial hyperpolarization and ATP depletion in patients with systemic lupus erythematosus. *Arthritis Rheum* 2002, 46:175-90.

33. Doisneau-Sixou SF, Sergio CM, Carroll JS, Hui R, Musgrove EA, Sutherland RL: Estrogen and antiestrogen regulation of cell cycle progression in breast cancer cells. *Endocr Relat Cancer* 2003, 10:179-86.

34. Kharat I, Saatcioglu F: Antiestrogenic effects of 2,3,7,8-tetrachlorodibenzo-p-dioxin are mediated by direct transcriptional interference with the liganded estrogen receptor. Cross-talk between aryl hydrocarbon- and estrogen-mediated signaling. *J Biol Chem* 1996, 271:10533-7.

35. Ali S, Coombes RC: Endocrine-responsive breast cancer and strategies for combating resistance. *Nat Rev Cancer* 2002, 2:101-12.

36. Shupnik MA: Crosstalk between steroid receptors and the c-Src-receptor tyrosine kinase pathways: implications for cell proliferation. *Oncogene* 2004, 23:7979-89.

37. Planas-Silva MD, Bruggeman RD, Grenko RT, Stanley Smith J: Role of c-Src and focal adhesion kinase in progression and metastasis of estrogen receptor-positive breast cancer. *Biochem Biophys Res Commun* 2006, 341:73-81.

38. Hiscox S, Jordan NJ, Smith C, James M, Morgan L, Taylor KM, Green TP, Nicholson RI: Dual targeting of Src and ER prevents acquired antihormone resistance in breast cancer cells. *Breast Cancer Res Treat* 2008.

39. Park SW, Zhen G, Verhaeghe C, Nakagami Y, Nguyenvu LT, Barczak AJ, Killeen N, Erle DJ: The protein disulfide isomerase AGR2 is essential for production of intestinal mucus. *Proc Natl Acad Sci U S A* 2009, 106:6950-5.

40. Hosokawa Y, Arnold A: Mechanism of cyclin D1 (CCND1, PRAD1) overexpression in human cancer cells: analysis of allele-specific expression. *Genes Chromosomes Cancer* 1998, 22:66-71.

41. Goplen D, Wang J, Enger PO, Tysnes BB, Terzis AJ, Laerum OD, Bjerkvig R: Protein disulfide isomerase expression is related to the invasive properties of malignant glioma. *Cancer Res* 2006, 66:9895-902.

42. Sullivan DC, Huminiecki L, Moore JW, Boyle JJ, Poulsom R, Creamer D, Barker J, Bicknell R: EndoPDI, a novel protein-disulfide isomerase-like protein that is preferentially expressed in endothelial cells acts as a stress survival factor. *J Biol Chem* 2003, 278:47079-88.

43. Jamerson MH, Johnson MD, Dickson RB: Of mice and Myc: c-Myc and mammary tumorigenesis. *J Mammary Gland Biol Neoplasia* 2004, 9:27-37.

44. Finn RS: Targeting Src in breast cancer. *Ann Oncol* 2008, 19:1379-86.

45. Mita AC, Mita MM, Nawrocki ST, Giles FJ: Survivin: key regulator of mitosis and apoptosis and novel target for cancer therapeutics. *Clin Cancer Res* 2008, 14:5000-5.

46. Pink JJ, Jordan VC: Models of estrogen receptor regulation by estrogens and antiestrogens in breast cancer cell lines. *Cancer Res* 1996, 56:2321-30.

47. Normanno N, Di Maio M, De Maio E, De Luca A, de Matteis A, Giordano A, Perrone F: Mechanisms of endocrine resistance and novel therapeutic strategies in breast cancer. *Endocr Relat Cancer* 2005, 12:721-47.

Figure legends

Figure 1: siRNA-mediated AGR2 knockdown impacts anchorage-dependent and anchorage-independent growth in breast cancer cell lines. T47D, ZR-75-1, MDA-MB-231, SK-BR-3 cells were transfected with negative control siRNA (iNC), AGR2 siRNA (iAGR2) or untransfected (UT). KSP (DKSP) and its corresponding control (DNC) was used as a transfection control. Results are expressed as a ratio of untransfected cells (±SD), n=3. **(a)** Detection of endogenous AGR2 in breast cancer cell line supernatants by IP-Western and whole cell lysates by Western. AGR2 knockdown was confirmed in lysates 72h after transfection. β−actin served as a loading control. **(b)** The impact of iAGR2 on anchorage-dependent growth was evaluated at 96h post-transfection using the Cell Titer Glo assay. Anchorage-independent growth assays were also used: (i) soft agar colony formation assay **(c)**, with Alamar blue as a readout; (ii) spheroid assay (D), where lysed spheroid LDH levels were representative of total cell number after 8 days; corresponding spheroid images were also captured. *P<0.05; **P<0.01; ***P<0.001.

Figure 2: AGR2 knockdown reduces cell proliferation in ER-positive breast cancer cells. Cell cycle profiles were analyzed by BrdU incorporation. Cells were pulse-labeled with 10uM BrdU 48h after transfection and analyzed for BrdU incorporation by FACS. Cells were gated on Sub G_1, G_0/G_1, S, and G_2/M populations. **(a)** T47D, **(b)** ZR-75-1, **(c)** MDA-MB-231, **(d)** SK-BR-3 cells.

Figure 3: AGR2 knockdown induces cell death. ZR-75-1 cells were collected 96h after AGR2 knockdown and analyzed for cell death by measuring ssDNA breaks using: **(a)** F7-26 staining by FACS analysis, and **(b)** alterations in mitochondrial membrane

potential by determining the ratio of JC-1_{red} to JC-1_{green} and represented as a ratio of the untransfected control (±SD), n=3. MG132 and CCCP served as apoptosis and depolarization controls, respectively. Cell death was investigated 96h after AGR2 knockdown in T47D cells by using: **(c)** Annexin V (AV) and propidium iodide (PI) and gated on normal (AV-/PI-), necrotic (AV-/PI+), early apoptotic (AV+/PI-) and late apoptotic/necrotic (AV+/PI+) cells; **(d)** and JC-1 staining, as previously described.

Figure 4: Target modulation of proliferation and survival proteins by AGR2. **(a)** Lysates 72h after transfection with non-targeting control (iNC) or AGR2 (iAGR2) were evaluated by Western blot for modulation of regulators of growth and survival. Note: some blots may be from different gels run with the same set of samples. **(b)** ZR-75-1 cells were treated for 6h with BSA (5ug/mL), Novus rhAGR2 (rhAGR2 (N)), or in-house rhAGR2 (rhAGR2(I)) and analyzed by Western blot for cyclin D1 induction. **(c)** ZR-75-1 cells were plated in 8-well chamber slides and treated with 5 ug/mL of BSA or rhAGR2 (I) for 6h. Cells were stained with cyclin D1 and mounting media containing DAPI was used. Images were taken using a fluorescent microscope and pseudo-colored in Adobe Photoshop. **(d)** Quantitation of cyclin D1 immunofluorescence images. The percentage of cells in each bin based on cyclin D1 intensity are represented (Bin 1=weakest staining; Bin 4=brightest staining). Results are expressed as the mean±SD, n=4.

Figure 5: Evidence of ER-AGR2 crosstalk. **(a)** ZR-75-1 cells were treated with vehicle control (DMSO) or E2 (10nM) for 24h analyzed by Western blot. Numbers above bands represent relative AGR2 induction with E2 treatment after quantitation and normalized to β-actin (Image J). **(b)** Lysates 72h after AGR2 knockdown were analyzed by Western

blot for ER. **P<0.01. Note: some blots may be from different gels run with the same set of samples.

Figure 6: ER-independent activities after AGR2 knockdown. T47D cells were transfected with iNC or iAGR2 and after 24h, cells were treated in combination with 4-hydroxytamoxifen (4-OHT) or ICI 182,780 (ICI) at doses of 100 nM or 1 uM. The growth inhibitory effects of combination treatments were assessed by Cell Titer Glo 96h after transfection **(a)**, or the level of target modulation at 72h by Western blot analysis **(b)**. **(c)** Modulation of p-Src was analyzed 72h after AGR2 knockdown. The kinetics of cyclin D1 and ER modulation were determined by Western blot and densitometric values of cyclin D1 and ER were calculated and normalized to β-actin (Image J) and represented as the mean±SD, n=3**.** *P<0.05; **P<0.01; ***P<0.001, antiestrogen and AGR2 knockdown combination versus AGR2 knockdown alone. Note: some blots may be from different gels run with the same set of samples.

Figure 7: Impact of rat anti-AGR2 Ab on cell growth and cyclin D1 in T47D cells. **(a)** Rat anti-AGR2 Ab were tested for AGR2 specificity using an ELISA directed against human AGR2 and human AGR3. Species cross-reactivity was also assessed using an ELISA directed against mouse AGR2. **(b)** After confirming Ab specificity, T47D cells were treated with an anti-AGR2 Ab (10ug/mL) for 48h or AGR2 siRNA for 72h and cyclin D1 modulation was examined by immunofluorescence. Cells were stained with cyclin D1 and mounting media containing DAPI was used. Images were taken using a fluorescent microscope and pseudo-colored in Adobe Photoshop. The isotype control Ab used for cyclin D1 staining was an anti-AGR2 Ab of the same isotype but was not shown to modulate cyclin D1 or have an impact on growth. **(c)** Cyclin D1 intensity was quantitated

using ImagePro and binned based on intensity and the percentage of cells in each bin based on cyclin D1 intensity are represented (Bin 1=weakest staining; Bin 4=brightest staining). **(d)** T47D, ZR-75-1 and MDA-MB-231 cells were treated for 5 days with 20 ug/mL anti-AGR2 Ab. The relative number of cells was quantitated using the MTT assay. Results are expressed relative to untreated sample for each cell line.

Additional files

Additional file 1: Supplementary file 1. Impact of AGR2 on breast cancer cell growth using AGR2 siRNA from multiple vendors. **(A)** T47D and MDA-MB-231 cells were treated with AGR2 siRNA from Invitrogen, Ambion and Dharmacon and their appropriate non-targeting controls. Ninety-six hours after transfection, Cell Titer Glo was used as a readout for relative cell number. Results are expressed relative to untransfected cells. **(B)** Whole cell lysates were isolated from T47D and MDA-MB-231 cells at 48h, 72h or 96h after transfection to confirm knockdown or AGR2 protein.

Additional file 2: Supplementary figure 2. Additional death assays after AGR2 knockdown in T47D cells. **(A)** F7-26 staining, a measure of ssDNA breaks, was measured 96h after AGR2 knockdown in T47D cells by FACS analysis. Hydrogen peroxide was used as a positive control for the assay. **(B)** Alterations in mitochondrial membrane potential 120h after AGR2 knockdown were assessed by determining the ratio of $JC\text{-}1_{red}$ to $JC\text{-}1_{green}$ and represented as a ratio of the untransfected control (±SD), n=3. MG132 and CCCP served as apoptosis and depolarization controls, respectively.

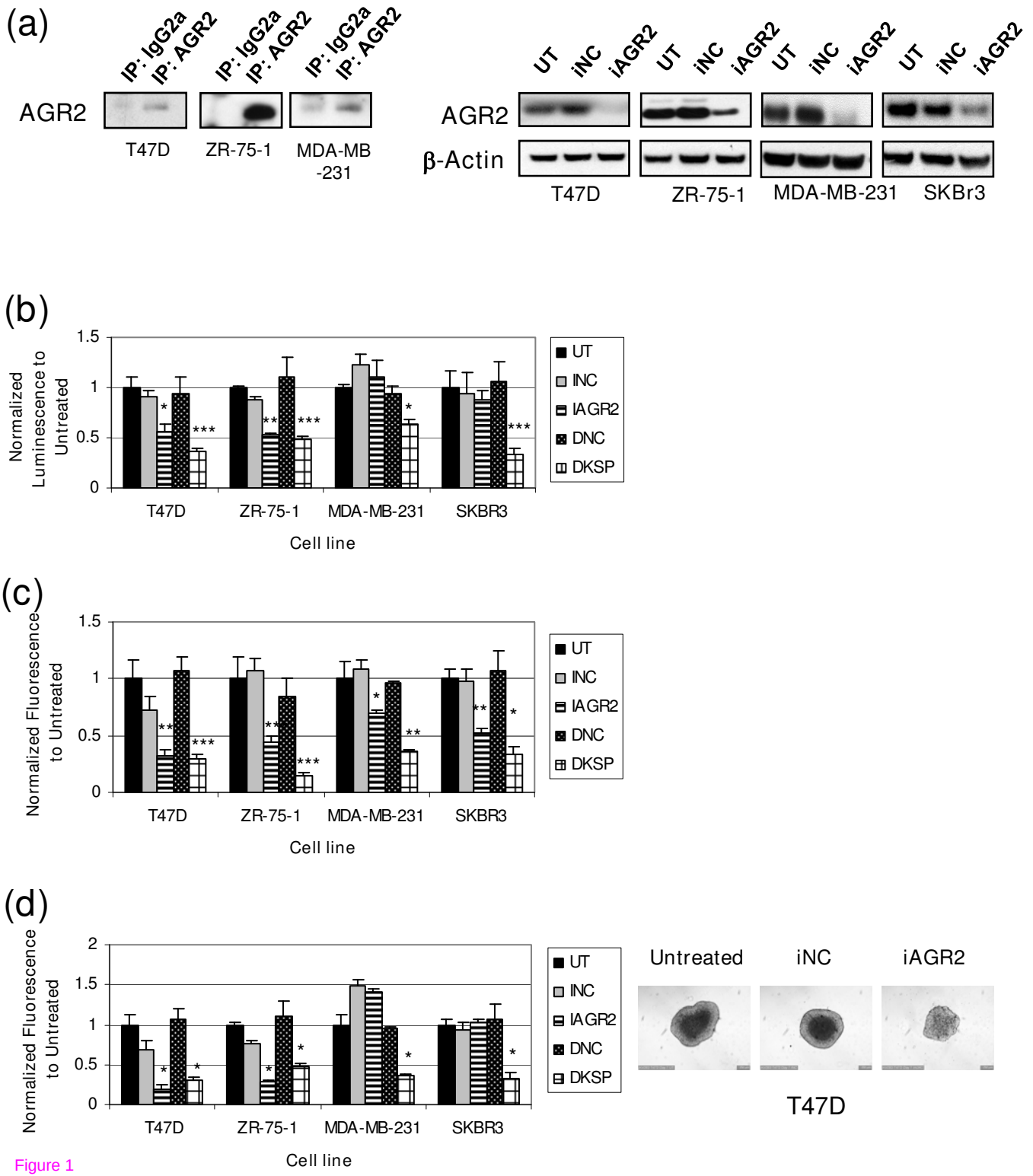
(a)
IP: IgG2a
IP: AGR2
AGR2
T47D
ZR-75-1
MDA-MB -231
UT
iNC
iAGR2
AGR2
β-Actin
T47D
ZR-75-1
MDA-MB-231
SKBr3
(b)
Normalized Luminescence to Untreated
1.5
1
0.5
0
UT
INC
IAGR2
DNC
DKSP
T47D
ZR-75-1
MDA-MB-231
SKBR3
Cell line
(c)
Normalized Fluorescence to Untreated
1.5
1
0.5
0
UT
INC
IAGR2
DNC
DKSP
T47D
ZR-75-1
MDA-MB-231
SKBR3
Cell line
(d)
Normalized Fluorescence to Untreated
2
1.5
1
0.5
0
UT
INC
IAGR2
DNC
DKSP
T47D
ZR-75-1
MDA-MB-231
SKBR3
Cell line
Untreated
iNC
iAGR2
T47D

Figure 1

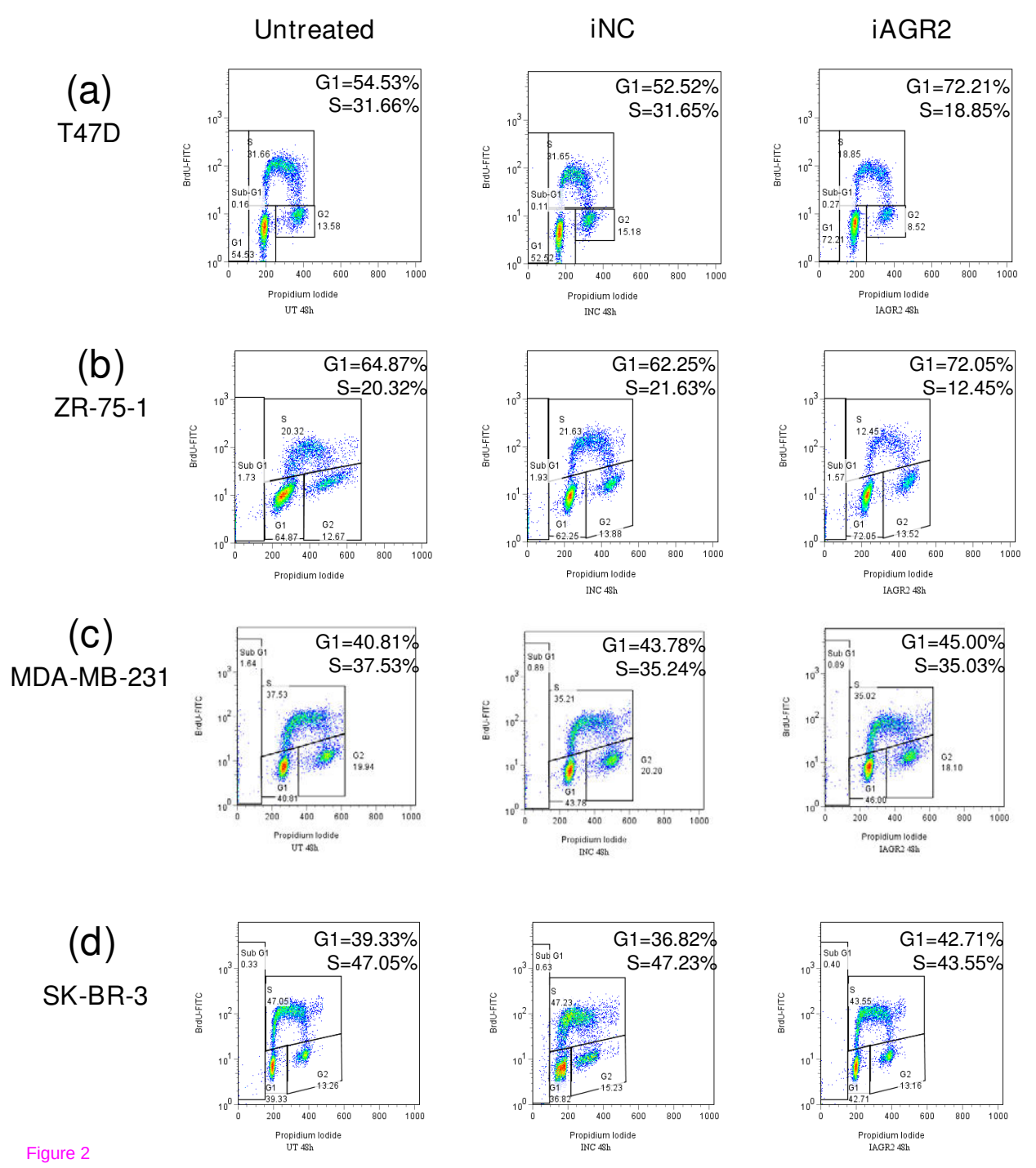
Untreated
iNC
iAGR2
(a)
T47D
G1=54.53%
S=31.66%
G1=52.52%
S=31.65%
G1=72.21%
S=18.85%
(b)
ZR-75-1
G1=64.87%
S=20.32%
G1=62.25%
S=21.63%
G1=72.05%
S=12.45%
(c)
MDA-MB-231
G1=40.81%
S=37.53%
G1=43.78%
S=35.24%
G1=45.00%
S=35.03%
(d)
SK-BR-3
G1=39.33%
S=47.05%
G1=36.82%
S=47.23%
G1=42.71%
S=43.55%
BrdU-FITC
Propidium Iodide
UT 48h
INC 48h
IAGR2 48h

Figure 2

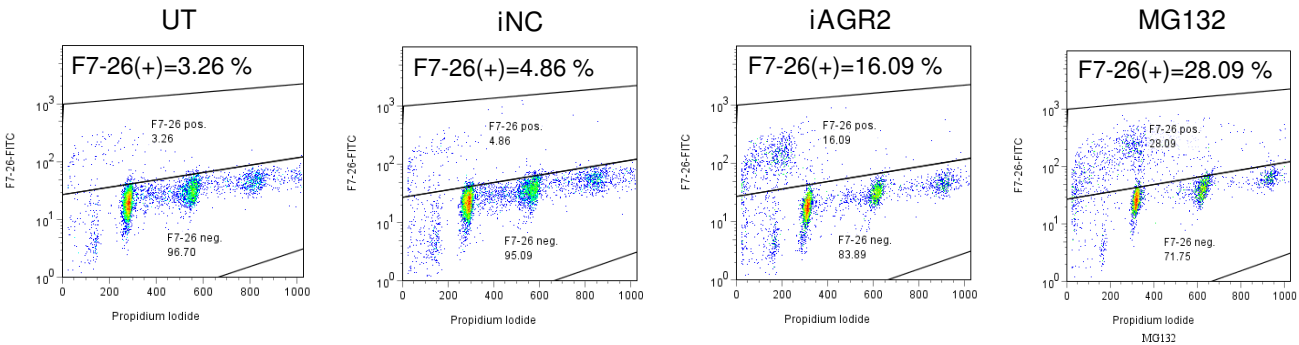
(a) ZR-75-1
UT
iNC
iAGR2
MG132
F7-26(+)=3.26 %
F7-26(+)=4.86 %
F7-26(+)=16.09 %
F7-26(+)=28.09 %
F7-26 pos. 3.26
F7-26 neg. 96.70
F7-26 pos. 4.86
F7-26 neg. 95.09
F7-26 pos. 16.09
F7-26 neg. 83.89
F7-26 pos. 28.09
F7-26 neg. 71.75
F7-26-FITC
Propidium Iodide
MG132

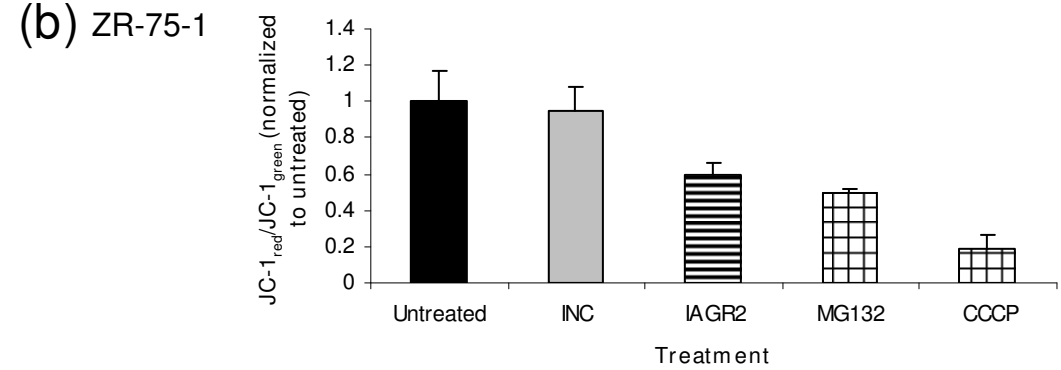
(b) ZR-75-1
JC-1red/JC-1green (normalized to untreated)
1.4
1.2
1
0.8
0.6
0.4
0.2
0
Untreated
INC
IAGR2
MG132
CCCP
Treatment

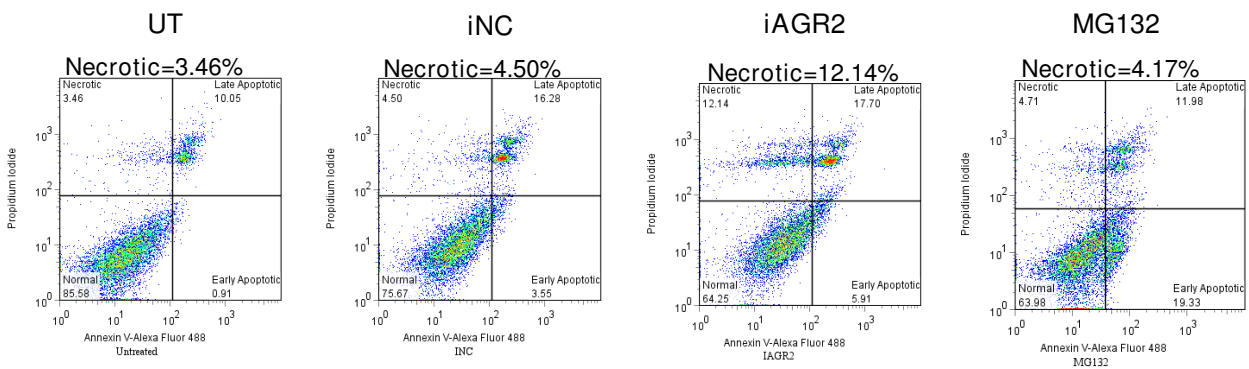
(c) T47D
UT
iNC
iAGR2
MG132
Necrotic=3.46%
Necrotic=4.50%
Necrotic=12.14%
Necrotic=4.17%
Necrotic 3.46
Late Apoptotic 10.05
Normal 85.58
Early Apoptotic 0.91
Necrotic 4.50
Late Apoptotic 16.28
Normal 75.67
Early Apoptotic 3.55
Necrotic 12.14
Late Apoptotic 17.70
Normal 64.25
Early Apoptotic 5.91
Necrotic 4.71
Late Apoptotic 11.98
Normal 63.98
Early Apoptotic 19.33
Propidium Iodide
Annexin V-Alexa Fluor 488
Untreated
INC
IAGR2
MG132

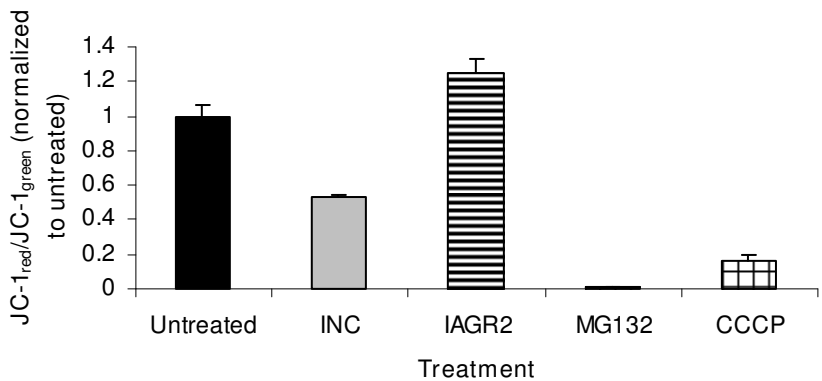
(d) T47D
JC-1red/JC-1green (normalized to untreated)
1.4
1.2
1
0.8
0.6
0.4
0.2
0
Untreated
INC
IAGR2
MG132
CCCP
Treatment

Figure 3

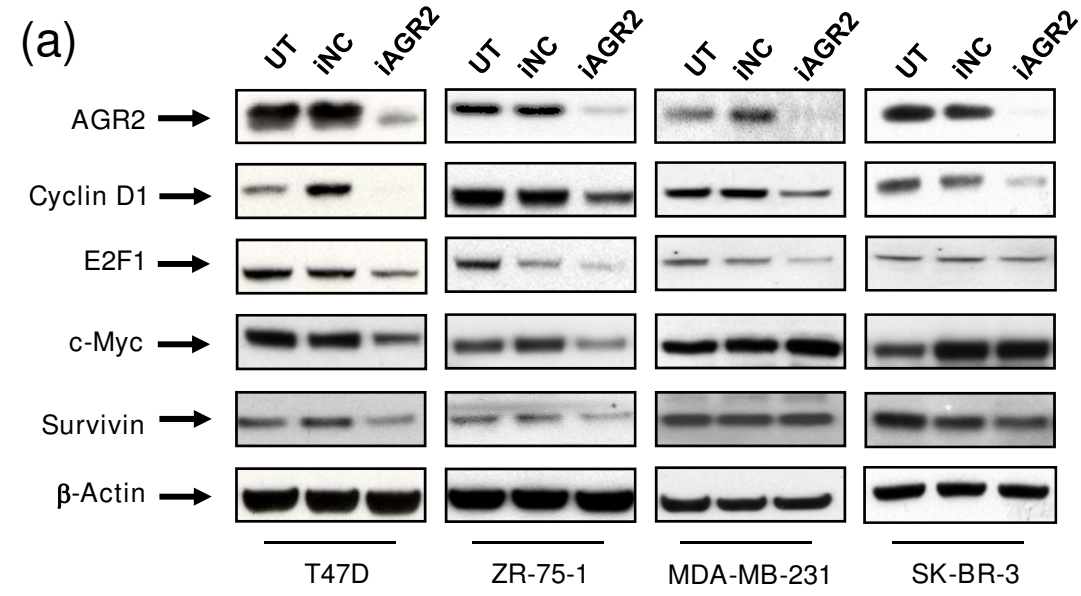
(a)
UT
iNC
iAGR2
AGR2
Cyclin D1
E2F1
c-Myc
Survivin
β-Actin
T47D
ZR-75-1
MDA-MB-231
SK-BR-3

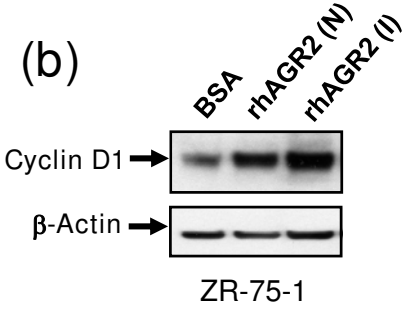
(b)
BSA
rhAGR2 (N)
rhAGR2 (I)
Cyclin D1
β-Actin
ZR-75-1

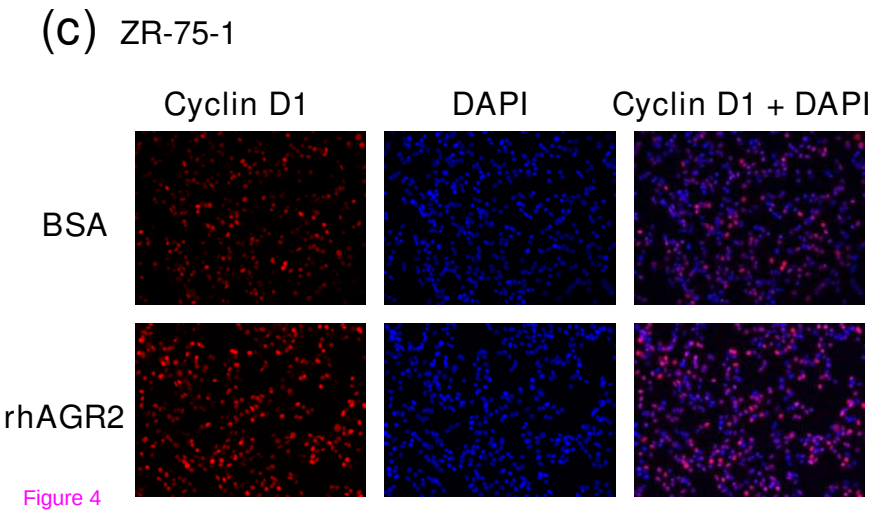
(c) ZR-75-1
Cyclin D1
DAPI
Cyclin D1 + DAPI
BSA
rhAGR2

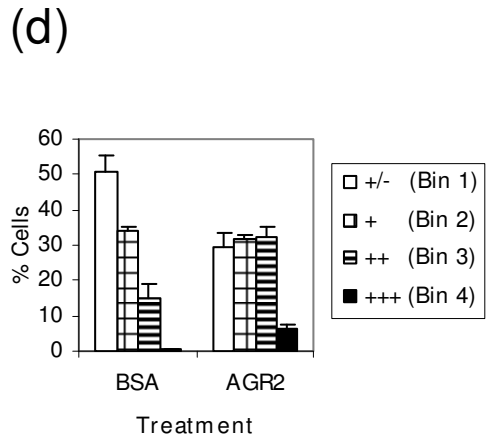
(d)
% Cells
60
50
40
30
20
10
0
BSA
AGR2
Treatment
+/- (Bin 1)
+ (Bin 2)
++ (Bin 3)
+++ (Bin 4)

Figure 4

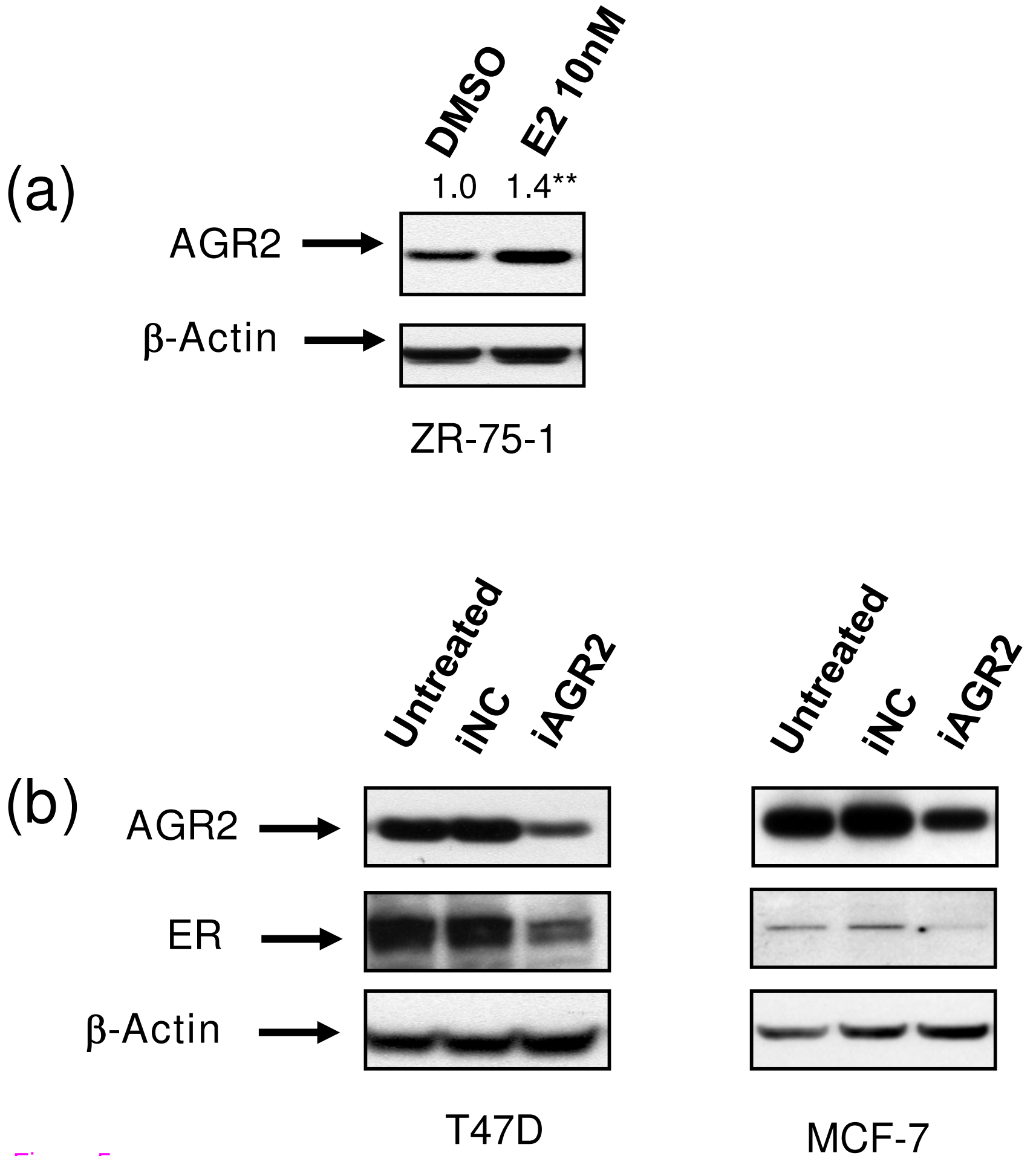
(a)
DMSO
E2 10nM
1.0
1.4**
AGR2
β-Actin
ZR-75-1
(b)
Untreated
iNC
iAGR2
Untreated
iNC
iAGR2
AGR2
ER
β-Actin
T47D
MCF-7

Figure 5

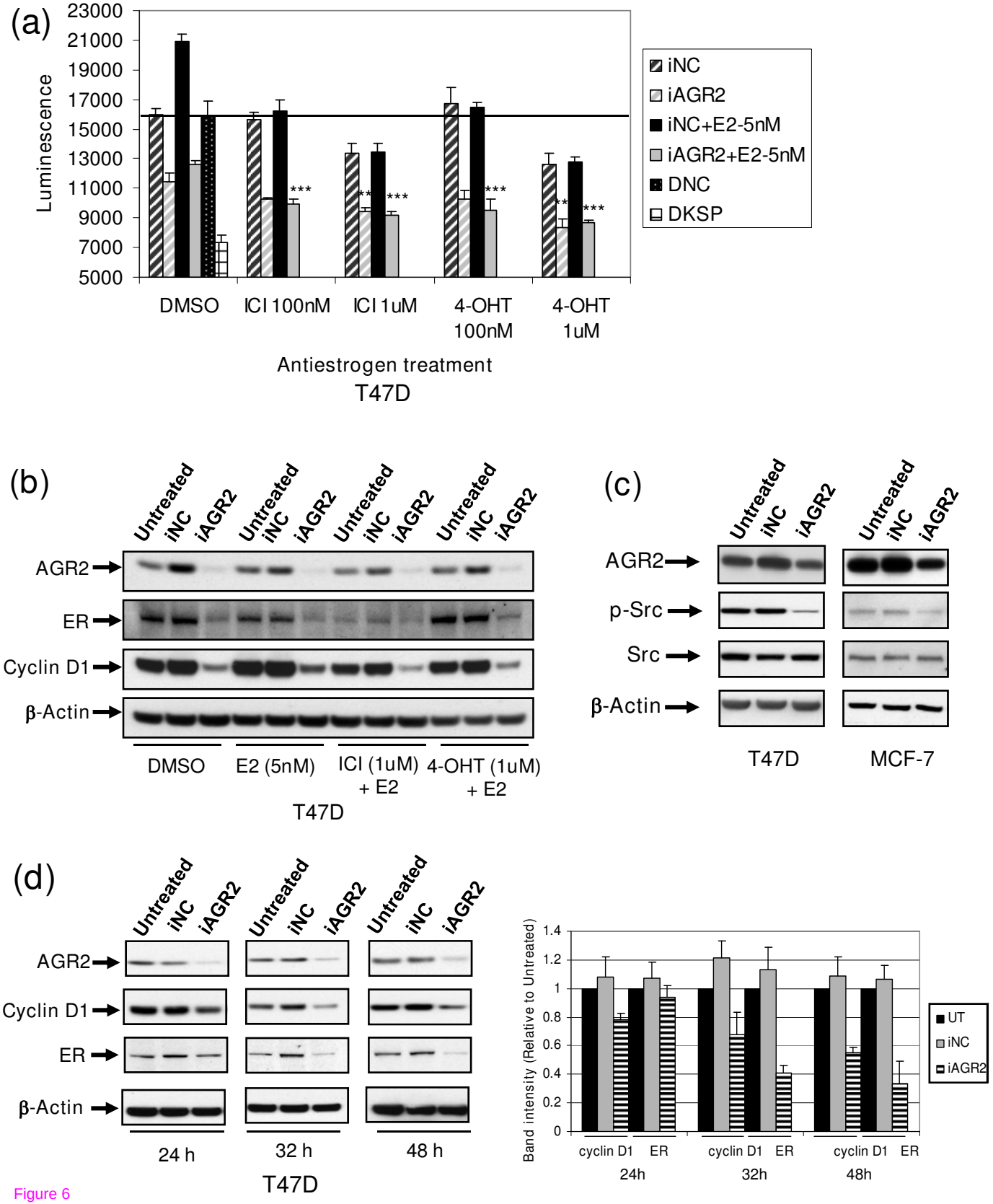
(a)
Luminescence
23000
21000
19000
17000
15000
13000
11000
9000
7000
5000
iNC
iAGR2
iNC+E2-5nM
iAGR2+E2-5nM
DNC
DKSP
**
***
DMSO
ICI 100nM
ICI 1uM
4-OHT 100nM
4-OHT 1uM
Antiestrogen treatment
T47D
(b)
Untreated
iNC
iAGR2
AGR2
ER
Cyclin D1
β-Actin
DMSO
E2 (5nM)
ICI (1uM) + E2
4-OHT (1uM) + E2
T47D
(c)
Untreated
iNC
iAGR2
AGR2
p-Src
Src
β-Actin
T47D
MCF-7
(d)
Untreated
iNC
iAGR2
AGR2
Cyclin D1
ER
β-Actin
24 h
32 h
48 h
T47D
Band intensity (Relative to Untreated)
1.4
1.2
1
0.8
0.6
0.4
0.2
0
cyclin D1
ER
24h
32h
48h
UT
iNC
iAGR2

Figure 6

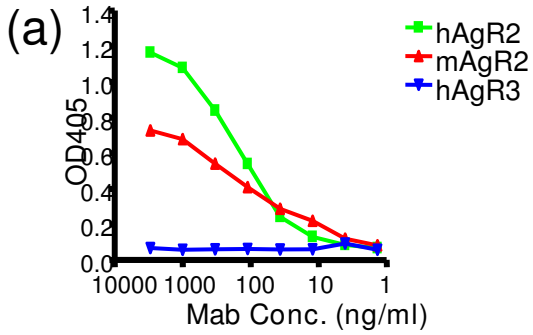
(a)
hAgR2
mAgR2
hAgR3
OD405
1.4
1.2
1.0
0.8
0.6
0.4
0.2
0.0
10000 1000 100 10 1
Mab Conc. (ng/ml)

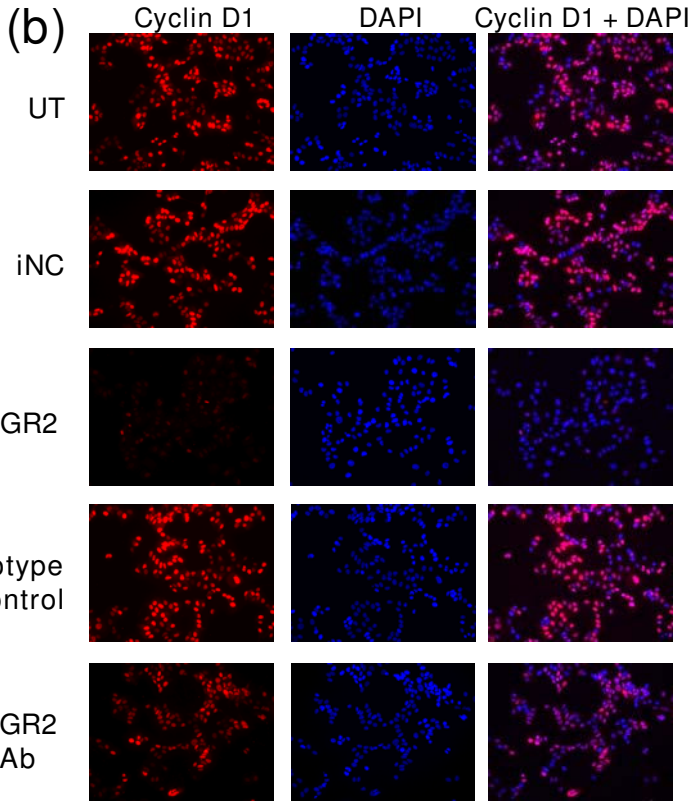
(b)
Cyclin D1
DAPI
Cyclin D1 + DAPI
UT
iNC
iAGR2
Isotype control
AGR2 Ab

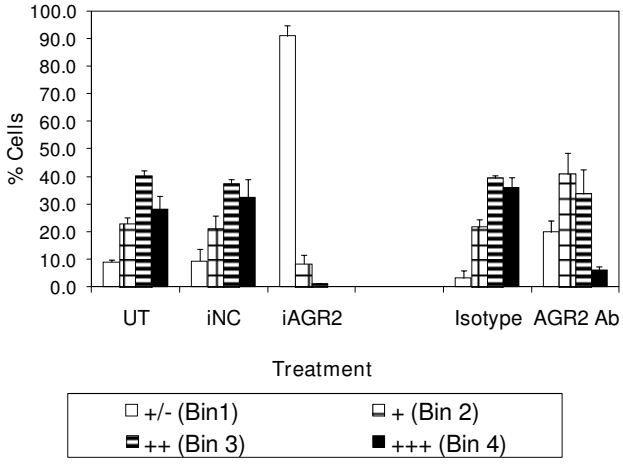
% Cells
100.0
90.0
80.0
70.0
60.0
50.0
40.0
30.0
20.0
10.0
0.0
UT
iNC
iAGR2
Isotype
AGR2 Ab
Treatment
+/- (Bin1)
+ (Bin 2)
++ (Bin 3)
+++ (Bin 4)

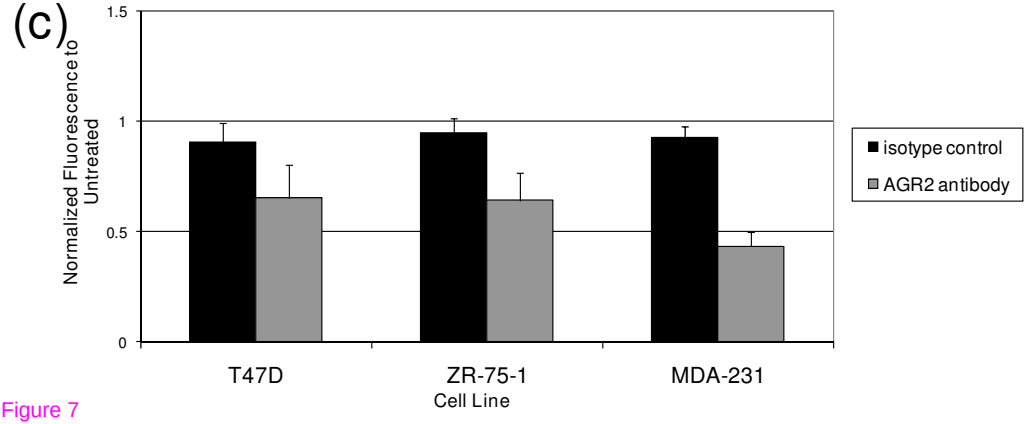
(c)
Normalized Fluorescence to Untreated
1.5
1
0.5
0
T47D
ZR-75-1
MDA-231
Cell Line
isotype control
AGR2 antibody

Figure 7

Additional files provided with this submission:

Additional file 1: supplementary figure1.ppt, 194K
http://breast-cancer-research.com/imedia/5629410413972395/supp1.ppt
Additional file 2: supplementary figure 2.ppt, 208K
http://breast-cancer-research.com/imedia/5966697313972395/supp2.ppt